Ketamine pharmacometrics

Kamp, J.

4

Pharmacokinetics of ketamine and its major metabolites norketamine, hydroxynorketamine and dehydronorketamine: a model-based analysis

Jasper Kamp
Kelly Jonkman
Monique van Velzen
Leon Aarts
Marieke Niesters
Albert Dahan
Erik Olofsen

British Journal Of Anaesthesia, 2020, Nov; 125(5):750-761

Ketamine, first synthetized in the early 1960s, is currently experiencing a renewed interest with applications in a variety of indications. It was initially developed as dissociative anesthetic and as a safer alternative to phencyclidine, causing less excitation upon emergence from anesthesia.[1] Presently, ketamine is increasingly used for treatment of acute (perioperative) pain, chronic neuropathic pain and therapy-resistant clinical depression. [1,2] While ketamine interacts with multiple receptor systems, its blockade of the *N*-methyl-D-aspartate receptor (NMDAR) is considered pivotal in producing anesthesia, pain relief and anti-depressant effects. [1,3] Ketamine is a racemic mixture (*RS*-ketamine) and is available in two commercial formulations. The racemic mixture (Ketalar) has been around for many years and is used in human and veterinary medicine. More recently (since 1997) the *S*-enantiomer (Ketanest) has been marketed in various European countries for the same indications as *RS*-ketamine, while in 2019 esketamine for intranasal administration (Spravato™) was registered in the United States and the European Union for treatment of therapy-resistant depression.[4-6] There are substantial differences in potency between the *S*- and *R*-ketamine isomers. For example, *S*-ketamine has a twofold greater anesthetic potency relative to the racemic,[7] the *R*-variant is three times more potent in its antidepressant effects than *S*-ketamine.[5]

Ketamine is extensively metabolized by cytochrome P450 enzymes, particularly by CYP2B6 and CYP3A4.[6,8] The main metabolic pathway involves demethylation to norketamine which is subsequently metabolized to dehydronorketamine (DHNK) and hydroxynorketamine (HNK).[1,9] These secondary metabolites, DHNK and HNK, were for a long time considered inactive or clinically irrelevant. However, recent studies showed activity of HNK in producing analgesia and antidepression.[5,10,11] Little is known about the pharmacokinetic behavior of these metabolites in humans. We found just one study, performed in nine patients with bipolar depression, that included DHNK and HNK in a pharmacokinetic analysis.[12] In the current study, we performed a population pharmacokinetic modeling study of ketamine and its metabolites (norketamine, DHNK end HNK) following administration of escalating doses of the racemic mixture and *S*-ketamine in twenty healthy volunteers. In this study both drugs were administered without and with a continuous infusion of the nitric oxide donor sodium nitroprusside (SNP). SNP was used to assess its ability to tame the schizotypal side effects of ketamine. The descriptive results of this study have been published before.[13] The main aim of this secondary analysis was to develop a mixed-effects population pharmacokinetic model for ketamine and its most important metabolites.

METHODS

Ethics and subjects

The current study is part of a large project on the efficacy of SNP in reducing the central and peripheral adverse effects of *RS*- and *S*-ketamine (*e.g.* drug high, schizotypal symptoms, and increased cardiac output). Secondary analyses were planned: (1) development of a population pharmacokinetic model of *RS*- and *S*-ketamine and their metabolites; (2) pharmacokinetic-pharmacodynamic modeling of the analgesic and psychotomimetic effects of *RS*- and *S*-ketamine ketamine; (3) pharmacokinetic-pharmacodynamic modeling of the effects of *RS*-and *S*-ketamine on cardiac output. Here we report on item (1). The study protocol was approved by the institutional review board of the Leiden University Medical Centre (CME, Leiden, the Netherlands) and the Central Committee on Research involving Human subjects (CCMO, The Hague, The Netherlands). The study was registered at the trial register of the Dutch Cochrane Center (www.trialregister.nl) under identifier 5359. All procedures were performed in compliance with the latest version of the Declaration of Helsinki and Good Clinical Practice guidelines.

Subject enrollment was performed as previously published.[13] In brief, healthy male subjects, aged 18-34 year and with a maximum body mass index of 30 kg m^{-2}, were recruited. For a complete list of exclusion criteria see Ref. 12. Importantly, subjects were excluded when they used any medication or herbs/vitamins in the 3 months before dosing. Additionally, they were not allowed to consume any caffeinated food or beverages in the 24 h before dosing or consume any grapefruit-containing food or beverages in the 7 days before dosing. No consumption of any food or drinks were allowed for 8 hours before dosing.

Study design

Drugs

The study had a double-blind, crossover and randomized design. All subjects were studied on 4 occasions, which were identical in their design, except for the drug combinations that were administered. On visits A and B, participants received escalating doses of intravenous *RS*-ketamine (Ketalar, Pfizer Pharma, Berlin, Germany), on visits C and D, they received escalating doses of *S*-ketamine (Ketananest-S, Eurocept BV, Ankeveen, the Netherlands). Additionally, subjects received intravenous placebo on visits A and C, and intravenous SNP (0.5 mg kg^{-1} min^{-1}) on visits B and D (the sequence of visits was randomized). Ketamine and SNP were infused via two distinct intravenous access lines placed on the ipsilateral hand and arm. *RS*-ketamine was administered according to the following infusion scheme: 0-60 min: 0.28 mg kg^{-1} h^{-1}, 60-120 min: 0.57 mg kg^{-1} h^{-1} and 120-180 min: 1.14 mg kg^{-1} h^{-1}; the equivalent *S*-ketamine infusion scheme was: 0-60 min: 0.14 mg kg^{-1} h^{-1}, 60-120 min: 0.28 mg kg^{-1} h^{-1} and 120- 180 min: 0.57 mg

kg^{-1} h^{-1}. The difference in dosing was based on observations that *S*-ketamine has twice the potency compared to *RS*-ketamine as based on a pilot study, in which psychedelic symptoms were evaluated after a 50 mg dose of both drugs.

Randomization and blinding

The sequence of the study visits was randomized using a computer-generated randomization list with a four-block design (www.randomization.org). The pharmacy was informed on the day prior to the study visit of the subject weight, subject and visit codes (#A-D). The pharmacy prepared the medication on the morning of the study visit according to Good Manufacturing Practice guidelines and the randomization list. Two syringes containing ketamine (*RS*-/*S*-ketamine) and placebo/SNP were dispensed to the research team in 50 mL syringes marked with the numerical subject and visit code and treatment (ketamine or SNP), ensuring full blinding of the research team. The research team remained blinded until all data were collected.

Blood sampling and analysis

Eight mL arterial blood samples were obtained on each occasion at predefined sampling times: t = 0 (baseline), and 2, 6, 30, 59, 62, 66, 100, 119, 122, 126, 150, 179, 182, 186, 195, 210 and 300 min after the start of ketamine infusion. Samples were drawn from an arterial line, which was placed in the radial artery of the arm opposite to the arm where the intravenous line was placed for drug infusion.

Plasma samples were analyzed in the laboratory of dr. Evan Kharasch (Washington University School of Medicine, St. Louis, MO) as extensively described by Rao et al.[13] An enantioselective assay was used for ketamine, norketamine and DHNK analyses. For HNK, total *S*- and *R*-concentrations were determined. For ketamine, norketamine and DHNK, the lower and upper limits of quantitation were 2.5 and 250 ng mL^{-1} and for HNK 5 and 500 ng mL^{-1}.

Population pharmacokinetic analysis

Model development

To account for the differences in molecular weight between ketamine and the metabolites, concentration data were converted from ng mL^{-1} to nmol mL^{-1}. Data analysis was performed in a stepwise fashion. First, the stereoselective ketamine data were analyzed using a three-compartment model, similar to the published model by Sigtermans et al.[14] Additionally, one and two compartment models were evaluated. Next, the best ketamine model was expanded by one to four metabolic delay compartments to model norketamine formation. Since no norketamine was administered, the volume of the central norketamine compartment (V_1) was not identifiable. It was therefore assumed that the volumes of the central ketamine and norketamine compartments were equal.

Since the kinetics of the central norketamine compartment could not be estimated from the data, we assumed that the amount of drug in the norketamine central compartment was in steady state (equilibrium) with respect to its peripheral and metabolism compartments.[14] Consequently, since the norketamine formation and elimination rates are then not both identifiable, the norketamine formation rate and ketamine elimination rate were assumed equal.[9,12,14] Different norketamine models with one, two or three norketamine compartments were fitted to the data. Finally, the optimal norketamine model was expanded with one to three metabolic compartments to model HNK and DHNK formation. Similar to norketamine, the volumes of DHNK and HNK V_1 were not identifiable and therefore set equal to the volume of ketamine V_1 and the sum of the DHNK and HNK formation rates was set equal to the norketamine elimination rate. Since no stereospecific HNK data were available, HNK formation was modeled as the sum from the separate *S*- and *R*-ketamine pathways.

To standardize the pharmacokinetic model parameters, and to add body weight (WT) information to the model, clearances were allometrically scaled to liters per hour at 70 kg by $CL = (WT/70)^{0.75}$. Furthermore, compartment volumes were scaled to 70 kg body weight by V = WT/70. Model selection was based on a significant decrease in objective function value (OFV) calculated as -2LogLikelihood (χ^2-test, with $p < 0.01$ considered significant) and by assessing the goodness of fit by visual inspection of data fits, and goodness of fit plots: normalized prediction distribution error *versus* time plots, normalized prediction distribution error *versus* predicted plots and predicted *versus* measured plots. Moreover, prediction-variance-corrected visual prediction checks (VPCs) were performed by simulating 1000 datasets based on the model parameters and comparing the simulated quantiles with those of the true data.

Statistical analysis

The data were analyzed in NONMEM version 7.4.3 (ICON Development Solutions, Hanover, Maryland). The M3 method for data censoring, as published by Beal et al., was used for data below the level of quantitation and data above the upper limit of the calibration curve.[15] The LAPLACE-I estimation algorithm was used to estimate model parameters. To account for interindividual and inter-occasion variability (IOV), random effects were included in the model with an exponential relation: $\theta_i = \theta \times \exp(\eta_i + \eta_{iov})$, where θ_i is the parameter for individual i, θ the population parameter, η_i is the random difference between the population and individual parameter and η_{iov} the difference between θ_i and θ due to inter-occasion variability. In addition, proportional and additive errors were evaluated for each separate analyte to account for residual variability. The proportional and combined proportional and additive error models were described by: $Y_{ij} = F_{ij} \times (1 + \varepsilon_{ij})$ and $Y_{ij} = F_{ij} \times (1 + \varepsilon_{1ij}) + \varepsilon_{2ij}$ respectively, where Y_{ij} is the j^{th} observed plasma concentration for individual i, F_{ij} is the corresponding model-prediction, and $_{ij}$ is

the residual error. The standard errors of the estimates (SEE) were based on NONMEM's covariance step without specifying a MATRIX option, so the default was used (i.e., the "Sandwich" matrix).

To test the effects of potential covariates the model, we performed a covariate search using an automated stepwise covariate screening algorithm (Stepwise Covariate Model building module from PsN).[16] Characteristics included in the covariate testing were: (i) analyte enantiomer (*S*- or *R*-isomer), (ii) placebo or SNP administration, and (iii) *S*-ketamine or *RS*-ketamine infused. Covariates were first tested by a forward search algorithm that sequentially added covariates that caused a significant drop in objective function value (OFV, $p < 0.01$) to the model. The relation between a covariate and a pharmacokinetic parameter was modeled as a linear relation with the formula: $\theta_i = \theta_{ref} \times (1 + \theta_{COV})$, where θ_{ref} is the typical parameter value for a subject with the reference category of the covariate and θ_{COV} the effect of belonging to the non-reference category. The covariate causing the largest decrease in OFV was included in the first step of the forward search, followed by the covariate causing the second largest decrease. This process continued until either no covariates were left for inclusion or when the remaining covariates were unable to cause a significant decrease in OFV. The final forward model was used for the backward selection, in which a similar strategy was used, although now covariates were removed from the model. Removed covariates that did not cause a significant worsening of the OFV ($p < 0.001$) were permanently excluded from the model. Covariates were maintained in the model when their removal caused a significant worsening of the OFV. This process continued until all covariates were excluded or until the covariates remaining in the model caused a significant worsening in OFV when removed.

Simulations

The clinical relevance of the covariates that were added to the model by Stepwise Covariate Model building, was evaluated by in simulation studies. The ketamine, norketamine, DHNK and HNK concentration time relationships of dose escalating ketamine infusions were simulated for a 70 kg individual and were performed using the RxODE package (version 0.8.0-9) for R studio (version 1.1.456, 2009-2018 RStudio, Inc). Three different conditions were simulated: *S*-ketamine after *S*-ketamine infusion, *S*-ketamine after *RS*-ketamine infusion and *R*-ketamine after *RS*-ketamine infusion. Furthermore, the effect size of SNP was evaluated by simulating each of these conditions without and with infusions of SNP. To evaluate ketamine and metabolite concentrations in a clinical scenario, plasma concentrations were simulated for a typical 70 kg individual, following a dose of 0.5 mg/kg *S*-ketamine or *RS*-ketamine infused in 40 minutes.

RESULTS

All 20 subjects completed the four visits without serious adverse events. Mean ± SD (range) subject body weight was 83 ± 9 (60-98) kg, height 186 ± 6 (175-193) cm, age 23 ± 2 (19-28) years and body mass index 24.0 ± 2.1 (19.5-28.4) kg m^{-2}. Complete concentration curves were obtained in all subjects, with the exception for one visit of one subject due to the inability to place the arterial line. A complete overview of the subject selection is shown in the consort flowchart (Supplemental figure 1). Ketamine, norketamine, DHNK and HNK concentrations are shown in Figure 1.

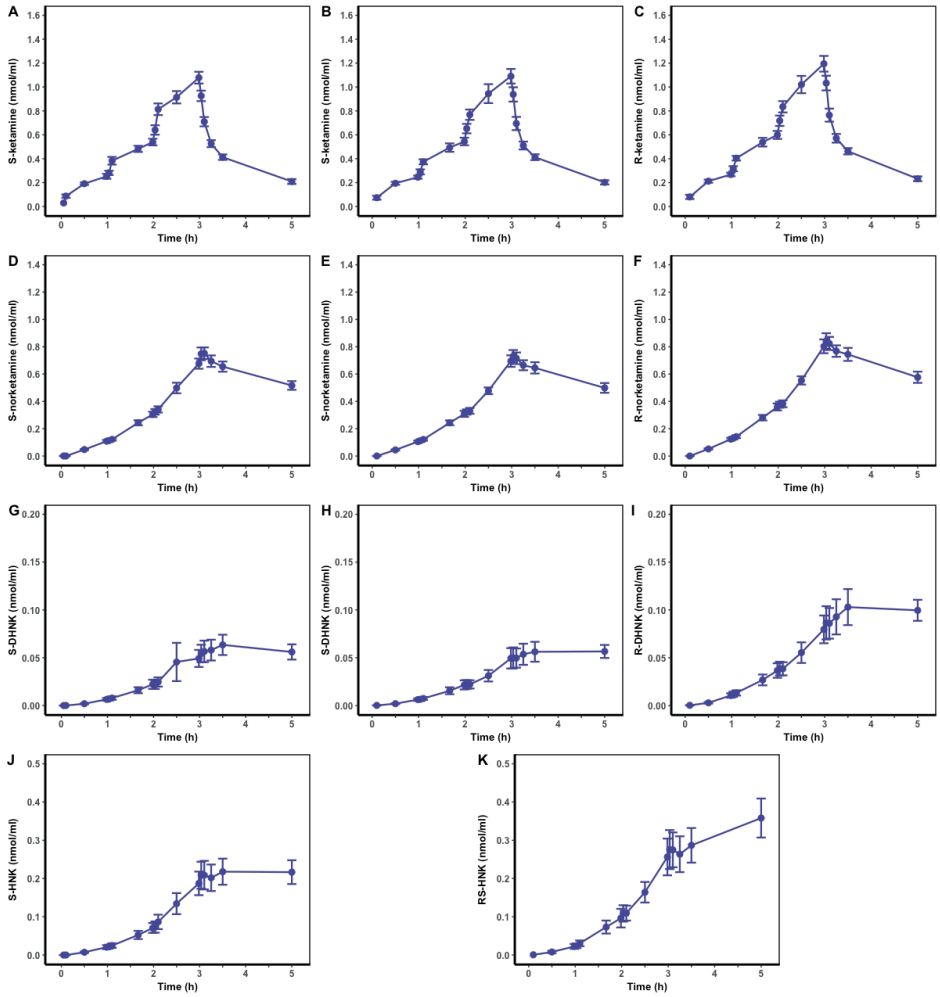

Figure 1. Mean plasma concentrations (+/- SE) of *S*-ketamine, *S*-norketamine and *S*-DHNK after esketamine (**A,D,G**); *S*-ketamine, *S*-norketamine and *S*-DHNK after racemic (**B,E,H**); *R*-ketamine, *R*-norketamine and *R*-DHNK after racemic ketamine administration (**C,F,I**) and total HNK plasma concentrations after racemic ketamine (**I**).

Peak concentrations

An overview of peak concentrations (C_{MAX}) with their respective times (T_{MAX}) are shown in Supplemental Table 1. Following racemic ketamine infusion, higher peak *R*- than *S*-enantiomer plasma concentrations were observed for ketamine, norketamine and DHNK. Importantly, the concentration difference between the enantiomers increased with each metabolic step (*i.e,* the enantiomer concentration difference was greater for DHNK than for norketamine). Metabolite peak concentrations were delayed relative to the ketamine peak concentrations (ketamine T_{MAX} = 170-173 min) by 17 min for norketamine (irrespective of formulation) and 80-120 min for DHNK; the delay in HNK peak concentration was 81 min following *S*-ketamine infusion and 69-72 min following racemic ketamine. Note however, that not all subjects reached their HNK and DHNK C_{MAX} within the sampling time (Fig. 1). For ketamine, 12% of measured plasma concentrations (n = 241) were below or above the lower and upper level of quantitation, for norketamine 6.6% (n = 127), for DHNK 30% (n = 580) and for HNK 14% (n = 149).

Structural pharmacokinetic model

The final model structure is shown in Figure 2. Ketamine pharmacokinetics were best described by a two-compartment model (ΔOFV = -6976). Adding significant covariates resulted in a further improvement of the ketamine model to an ΔOFV of -7130 points (Table 1). Norketamine was best modelled with two norketamine disposition compartments (ΔOFV = -8635). Extending the model by adding two metabolic delay compartments for the norketamine formation, improved the model by 70 points. The model was further improved by 702 points after addition of covariates. It was not possible to estimate the separate norketamine fractions that were metabolized to DHNK and HNK. We considered three different conditions with different fixed fractions for the DHNK and HNK formation 30%:70%, 40%:60% and 50%:50% (DHNK%:HNK%) from norketamine to overcome structural parameter un-identifiability.

Based on the observed plasma concentrations (Fig. 1 and Supplemental Table 1), we assumed that the fraction 30%:70% was most realistic, and present the data analysis using this conversion rate. DHNK was best modeled with one metabolic delay compartment and one disposition compartment (ΔOFV = -9212). The covariates caused a further OFV drop of 2349 points. In contrast, one HNK metabolic compartment coupled to one HNK disposition compartment showed a clear discrepancy in the elimination phase in the VPC. A model with two disposition compartments without a metabolic compartment solved this problem (ΔOFV = -5106). Adding covariates further improved the model by 26 points.

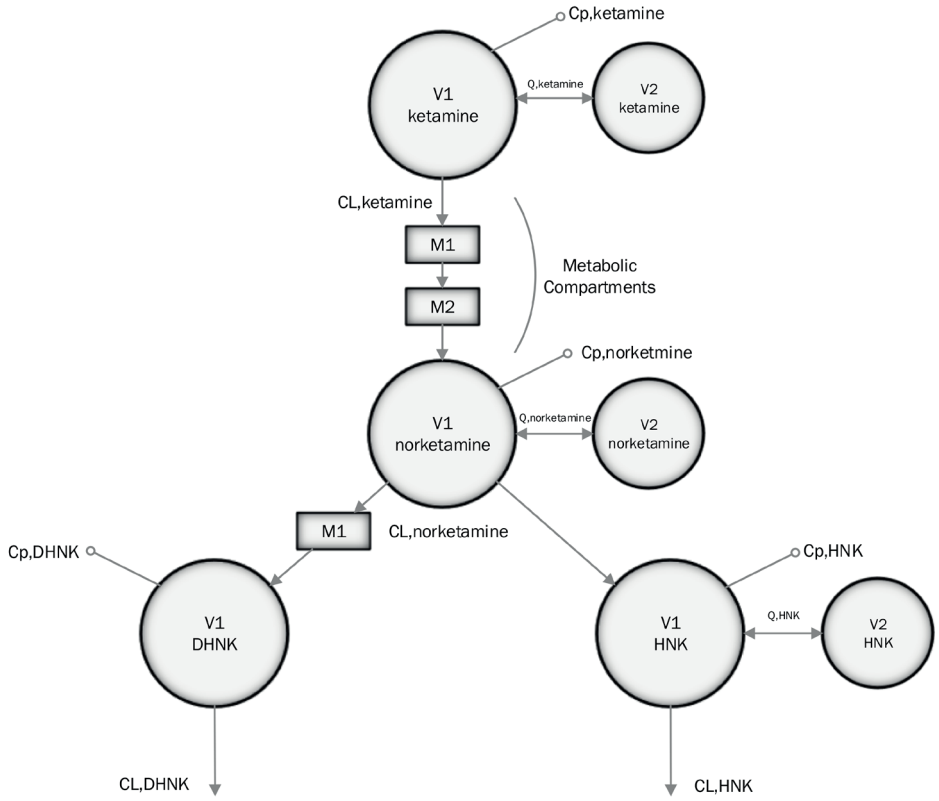

Figure 2. Schematic overview of the final pharmacokinetic model for ketamine, norketamine, DHNK and HNK. V1,ketamine; V2,ketamine; CL,ketamine and Q,ketamine represent the central and peripheral ketamine compartments and the ketamine elimination and intercompartmental clearances respectively. Norketamine formation is modelled via 2 metabolic compartments (M1-2). V1,norketamine; V2,norketamine; CL,norketamine and Q,norketamine represent the central and peripheral norketamine compartments and norketamine elimination and intercompartmental clearances respectively. DHNK formation from norketamine was modeled via one metabolic compartment (M1). DHNK was modeled with one disposition compartment (V1,DHNK) with elimination clearance CL, DHNK. No metabolic compartments were used for the formation of HNK from norketamine. V1, HNK and V2,HNK represent the central and peripheral HNK compartments respectively with elimination clearance CL, HNK and intercompartmental clearance Q,HNK.

Pharmacokinetic model parameters

To get an indication of the, best, median and worst fits based on the coefficient of determination (R^2), model fits are given in Figure 3 for pooled ketamine (Fig. 3A-C), norketamine (Fig. 3D-F), DHNK (Fig. 3G-I) and HNK (Fig. 3J-L) data sets. Goodness of fit plots are given in Supplemental Figure 2, showing a small misfit for *R*- and *S*-ketamine (panels A and B); the model slightly overestimates ketamine plasma concentrations at the lower concentration ranges. Otherwise, data fits and goodness of fit plots indicate that the

Table 1. Population pharmacokinetic model parameters

	Parameter estimates		
	Typical parameter value ± SEE (%CV)	**Inter-individual variability ± SEE (%CV)**	**Inter-occasion variability ± SEE (%CV)**
Ketamine			
V_1 (L/70 kg)	25.8 ± 1.5 (6)	20.2 ± 4.85% (24)	20 ± 2.60% (13)
V_2 (L/70 kg)	115 ± 5.8 (5)	17.6 ± 2.82% (16)	-
CL (L/h at 70 kg)	106.8 ± 3.2 (3)	10.7 ± 1.5% (14)	10.3 ± 0.93% (9)
Q (L/h at 70 kg)	126 ± 6.3 (5)	20.5 ± 5.13% (25)	-
additive error (nmol/L)	38.9 ± 2.3 (6)	-	-
proportional error	0.108 ± 0.006 (6)	-	-
Covariates			
CL (% decrease when R-ket)	11.5 ± 0.58 (5)	-	-
CL (% increase when SNP)	9.2 ± 2.22 (24)	-	-
Q (% increase when SNP)	21.6 ± 5.18 (24)	-	-
Norketamine			
V_2 (L/70 kg)	240 ± 19.2 (8)	25.2 ± 4.28% (17)	36 ± 3.24% (9)
CL (L/h at 70 kg)	59.9 ± 3.6 (6)	-	-
Q (L/h at 70 kg)	196.2 ± 9.8 (5)	19.7 ± 3.35% (17)	24.2 ± 2.42% (10)
MTT (min)	26.6 ± 2.1 (3)	-	-
additive error (nmol/L)	-	-	-
proportional error	0.12 ± 0.005 (4)	-	-
Covariates			
CL (% decrease when R-norketamine)	26.9 ± 2.15 (8)	-	-
Q (% decrease when R-norketamine)	22.1 ± 2.43 (11)	-	-
Dehydronorketamine			
CL (L/h at 70 kg)	185.4 ± 20.39 (11)	44.1 ± 7.5% (17)	21.2 ± 2.12% (10)
MTT (min)	36.9 ± 2.95 (8)	36.9 ± 29.52% (8)	-
additive error (nmol/L)	1.82 ± 0.25 (14)	-	-
proportional error	0.141 ± 0.01 (7)	-	-
Covariates			
CL (% decrease when R-DHNK)	49.3 ± 3.94 (8)	-	-
MTT (% increase when racemic ketamine)	20 ± 12.2 (61)		
MTT (% decrease when R-DHNK)	16.1 ± 13.36 (83)		
Hydroxynorketamine			
V_2 (L/70 kg)	216 ± 41 (19)	-	-
CL (L/h at 70 kg)	76.2 ± 20.60 (27)	86 ± 21.5% (25)	62.4 ± 7.49% (12)
Q (L/h at 70 kg)	218.4 ± 45.90 (21)	64.4 ± 23.18% (36)	34.6 ± 6.23% (18)
additive error (nmol/L)	5.88 ± 1.2 (20)	-	-
proportional error	0.249 ± 0.01 (8)	-	-
Covariates			
Q (% increase when Racemic)	114 ± 39.9	-	-

SEE = standard error of the estimate; %CV = % coefficient of variation, calculated as the SEE / typical parameter value * 100; V_1 = volume central compartment; V_2 = volume peripheral compartment, CL = elimination clearance, Q = intercompartmental clearance, MTT = mean transition time. Central compartment volumes (V_1) for NKT, DHNK and HNK were assumed to be equal to that of KET.

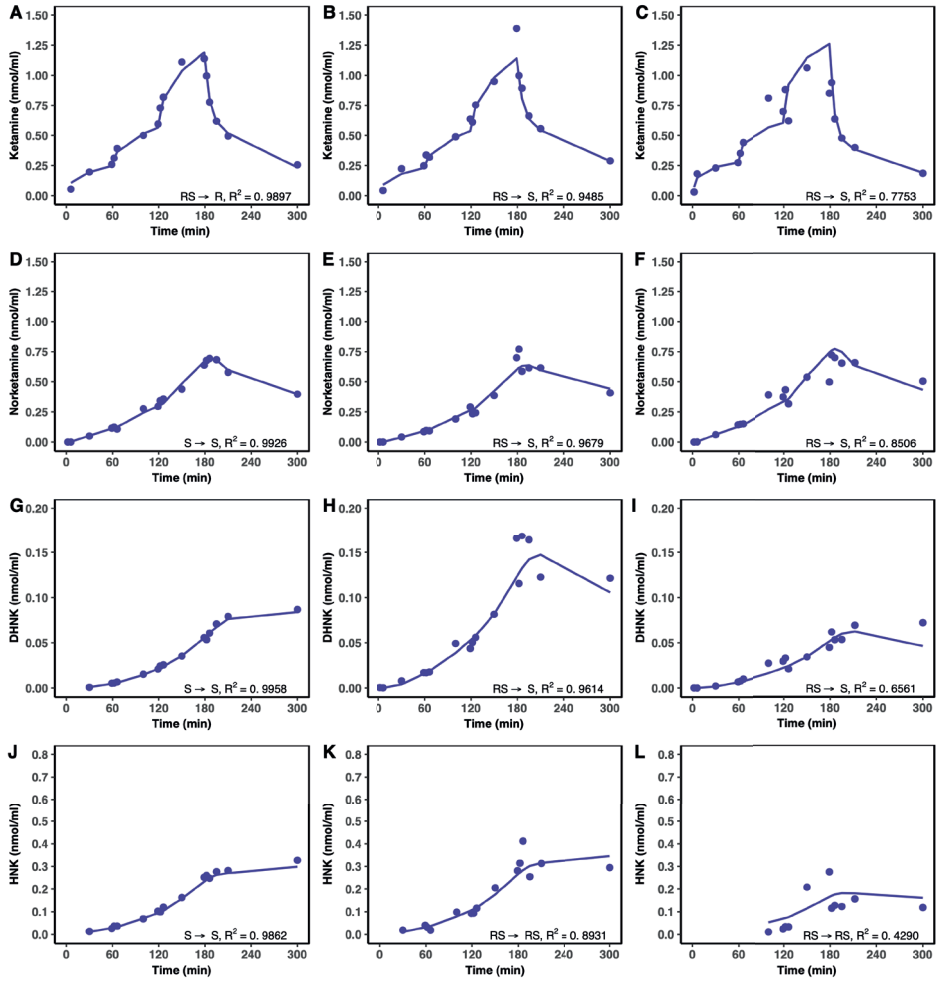

Figure 3. Pharmacokinetic model fits. Best (left panels), median (center panels) and worst (right panels) fits for pooled ketamine (**A-C**), norketamine (**D-F**), DHNK (**G-I**) and HNK (**J-L**) data sets. The circles represent the true data. The lines are the model fits.

model adequately describes the data. The Visual Predictive Checks are given in Supplemental Figures 3-6. No overt misfits became apparent with 95% of measured data points within the 95% prediction intervals for the simulated ketamine, norketamine and HNK data; for DHNK some of the data points at the highest dose (180 min) lie above the 95% prediction interval. The simulated 95% prediction intervals of the proportions of the data under the lower limit of quantitation (LLOQ) or above the upper limit of quantitation (ULOQ) were generally in agreement with the observed proportions. For HNK, a small misfit was observed for the proportion of the data under the LLOQ at the begin of the sampling scheme (Supplemental figure 6B). The observed proportion of

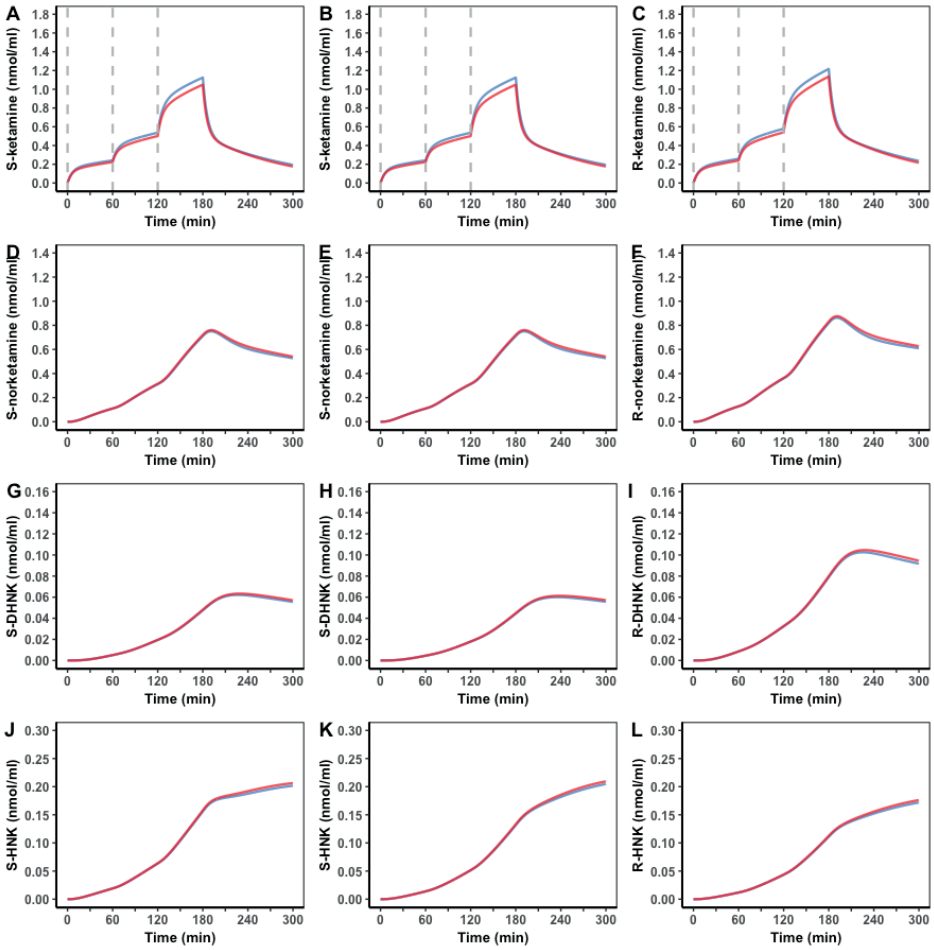

Figure 4. Model simulations. Simulated concentration time profiles for a 70 kg individual after receiving escalating esketamine infusions (left panels) or racemic ketamine (center and right panels) and with concomitant placebo administration (blue lines) or with SNP (red lines). Gray lines indicate the start of each ketamine dose.

0.5 was due to the limited number of samples in which HNK could be detected (n = 2). Of these two samples, one sample was above the LLOQ and one sample was under the LLOQ and could therefore not be reliably quantified.

Parameter estimates and included covariates are given in Table 1. The *R*-enantiomers of ketamine, norketamine and DHNK had a 11.5-49.3% lower elimination clearance than their *S*-variants. For ketamine, concomitant administration of SNP was associated with a 9.2% increase in elimination and a 21.6% increase in intercompartmental clearance. Since HNK plasma levels were not measured stereo-selectively, only the effects of the formulation (racemic- and *S*-ketamine) and concomitant infusion of SNP or placebo

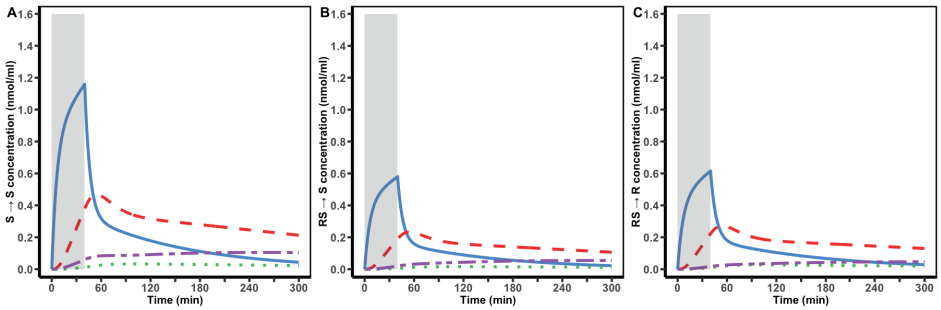

Figure 5. Simulations in clinical context. Concentration time profiles of ketamine, norketamine, DHNK and HNK (blue, red, green and purple lines respectively) after 0.5 mg/kg esketamine (**A**) or racemic ketamine (**B, C**) in a 70 kg individual. Note that, since racemic ketamine consists for 50% out of *S*-ketamine and for 50% out of *R*-ketamine, peak concentrations for *S*-ketamine and *R*-ketamine after racemic ketamine (**B,C**) are approximately half of the *S*-ketamine peak concentration after esketamine. Highlighted area indicates duration of infusion.

could be tested. SNP had no effect on HNK pharmacokinetics. Following *RS*-ketamine infusion the HNK intercompartmental clearance increased by 114% relative to just *S*-ketamine infusion.

Simulations

In addition to the automated covariate search, the exploration of the importance of the included covariates was assessed through simulations. The effect of the two formulations (racemic versus *S*-ketamine) and co-administration of SNP or placebo on plasma concentrations was simulated using the same infusion paradigm as in the experimental study (Fig. 4). Overall, the effects of the covariates were small.

Administration of SNP caused small (< 10%) reductions in peak *S*- and *R*-ketamine concentrations, irrespective of the formulation (red *versus* blue (placebo) lines in Fig. 4A-C), which is explained by the higher ketamine clearances during SNP administration. However, this difference was not seen for the metabolites. The formulation had no effect on the *S*-ketamine plasma concentrations. Peak *R*-ketamine concentration following racemic ketamine infusion was higher than the *S*-ketamine concentrations following racemic or *S*-ketamine infusion. This effect was about 10%, which is due to the lower *R*- than *S*-ketamine clearance. Similarly, peak *R*-norketamine and *R*-DHNK concentrations were higher than the *S*-variant following racemic ketamine infusion by factors 1.2 and 1.7, respectively. Although no stereo-selective data were obtained for HNK, the simulations (that considered *S*-HNK formation following *S*-ketamine infusion; Fig. 4J) suggest that following racemic ketamine infusion, the *R*-enantiomer was produced slower with a lower peak concentration than the *S*-variant (Fig. 4K and L). The simulations for the clinical scenario (Fig. 5) show plasma concentrations of norketamine (red line) and HNK (purple line) that eventually exceed ketamine concentrations.

DISCUSSION

In this study the plasma concentrations of ketamine and three of its most important metabolites, norketamine, DHNK and HNK, following escalating doses of racemic ketamine and esketamine, were quantified and analyzed using a population pharmacokinetic model. While often not considered clinically relevant, the importance of the metabolite HNK and to a lesser extent DHNK came to light in recent years, as these metabolites may be responsible for a (large) part of the antidepressant properties of ketamine.[5,11] Additionally, HNK has been shown to produce analgesia in rodent pain models, without the schizotypal side effects that obstruct the use of ketamine in chronic pain treatment.[10] An extensive understanding of the pharmacokinetics of ketamine and its metabolites is therefore of importance and will not only increase our knowledge of the pharmacokinetics of ketamine and its metabolites *per se*, but will also allow the design of precise infusion schemes for specific indications.

Ketamine is extensively metabolized in the liver.[17] The major metabolic pathway is through *N*-demethylation by hepatic enzymes CYP2B6 and CYP3A4 into norketamine.[6,8] Norketamine is subsequently metabolized to HNK by CYP2B6 and CYP2A6 enzymes or to DHNK by CYP2B6 (dehydrogenation). Furthermore, some DHNK may be produced from HNK through dehydration. Minor metabolic pathways that produce low abundance metabolites include hydroxylation of ketamine to hydroxyketamine or hydroxyphenylketamine.[11] Given the relative unimportance of these minor pathways, we modelled the major metabolic ketamine pathway and assumed that DHNK and HNK are both produced from norketamine in a 30:70 ratio. The resultant pharmacokinetic model (Fig. 2) was able to adequately describe the concentration time data of the stereoisomers of ketamine, norketamine and DHNK, and the sum of *R*- and *S*-HNK. Total HNK was modelled as we were unsuccessful in measuring the individual HNK stereoisomers. Still, we were able to predict *S*- and *R*-HNK formation in our simulations (Fig. 4K and L). We did not model DHNK formation from HNK as we assumed that just minute quantities of HNK were transformed into DHNK. Additionally, adding this metabolic pathway would have increased the complexity and therefore decreased stability of the model with consequently less reliable parameter estimates.

Our analysis indicates major differences in *S*- and *R*-enantiomer pharmacokinetics, irrespective of their origin, with significant higher concentrations of *R*-ketamine, *R*-norketamine and *R*-DHNK than the corresponding *S*-enantiomers (Fig. 1). This corresponded with an up to 50% reduced elimination clearance of the *R*- compared to the *S*-enantiomers. It is generally accepted that *S*-enantiomer metabolism is favored over *R*-enantiomer metabolism and is partly explained by the higher affinity of the CYP3A4 enzyme for *S*-ketamine. [5,18-21] Similar *S*- and *R*-enantiomer profiles were reported by Zhao et al.[11] They studied nine patients with treatment-resistant bipolar depression

following daily treatment with 0.5 mg/kg racemic ketamine given over 40 min, on three subsequent days. Zhao et al. analyzed concentration-time data during the initial 230 min following RS-ketamine administration as well as on the subsequent 3 days post infusion (in total 9 samples per subject were obtained) and constructed a population pharmacokinetic model that was made up of three ketamine, two norketamine and single HNK and DHNK compartments (no metabolism compartments were included). Similar to our data they observed an S:R concentration ratio < 1 for ketamine and DHNK, while no enantioselectivity was observed for norketamine. Alike our analysis, only total HNK was measured in the study of Zhao et al.[11] In contrast to our study, they observed that DHNK was the main metabolite in 4 of their subjects, norketamine in 3 and HNK in 2 subjects. In our study, total plasma HNK concentrations were approximately two times higher than the sum of *S*-and *R*-DHNK, which suggests that HNK formation is favored over DHNK formation during the first 5 hours following ketamine administration. Possibly the higher DHNK production observed by Zhao et al. was related to the longer sampling times.

A clinical important observation from the simulation study (Fig. 5) is that following a similar ketamine dose of 0.5 mg/kg given over 40 min (the dose used in the treatment of therapy-resistant depression), racemic ketamine HNK plasma concentrations are higher than following *S*-ketamine administration, *i.e.* the sum of *R*- and *S*-HNK concentrations after racemic ketamine exceeds *S*-HNK concentrations after *S*-ketamine administration. This suggests that when higher HNK concentrations are needed to improve treatment efficacy, the racemic formulation is to be preferred over *S*-ketamine. Additionally, from the simulation we infer lower *R*- than *S*-HNK concentrations, which we attribute to the slower formation of *R*-HNK. In rats, Moaddel et al. show higher (2*S*,6*S*)-HNK concentrations after *S*-ketamine infusion compared to (2*R*,6*R*)-HNK after *R*-ketamine infusion.[22] These data agree with our simulation data. However, a major limitation of our study is the restriction of HNK concentration data to 5 hours following the start of ketamine infusion. As a consequence, we may have missed peak HNK data occurring at later times. Hence, we cannot draw definite conclusions regarding a possible difference in *R*- and *S*-HNK pharmacokinetics in our data set.

Previous studies suggested differences in *S*-ketamine pharmacokinetics after administration *S*-ketamine *vs* racemic ketamine, due to the inhibition of *S*-ketamine metabolism by the *R*-enantiomer.[20] We were unable to detect significant differences in *S*-ketamine pharmacokinetics after either formulation. Hence, the clinical relevance of formulation (*i.e.* a formulation with or without *R*-ketamine) on *S*-ketamine pharmacokinetics therefore remains debatable.

In two arms of the study, we infused SNP. This was done to evaluate a possible modifying effect of SNP on the ketamine-induced schizotypal effects.[13] Additionally, SNP may reduce blood pressure elevations that coincide with ketamine treatment due

to ketamine-induced sympathoexcitation.[13] Importantly, SNP will cause vasodilation that may lead to increased distribution of ketamine. The observed increases in terminal and intercompartmental clearances were moderate (effect on ketamine CL and Q 9% and 22%, respectively) and were restricted to ketamine. Based on the simulations (Fig. 4), the effect of SNP on the complete pharmacokinetic picture seems limited. This further supports our hypothesis that the mitigating effect of SNP on psychotomimetic side effects of racemic ketamine is not pharmacokinetically driven but is related to the restoration of ketamine-induced depletion of intracellular nitric oxide, which restores neuroprotective effects from NMDAR activation.

The study has several limitations that warrant further commenting. First, the central volumes of distribution for all metabolites were set equal to the ketamine central volume of distribution. This was needed due to non-identifiability of these metabolite compartments. This might introduce bias to the estimation of metabolite clearances and peripheral compartment volumes. Administration of the metabolites or measurement of (glucuronide)-metabolites in urine could help solve this problem. However, norketamine, DHNK and HNK are currently not available for human use. Second, we were unable to estimate the parent fraction converted into metabolites. In agreement with other studies, we assumed that ketamine was fully transformed into norketamine.[9,12,14] This assumption may have influenced the parameter estimates of the formation of secondary metabolites from norketamine. The assumption of a 30%:70% ratio (DHNK:HNK) is based on the measured plasma concentrations and was needed to overcome structural parameter un-identifiability. Although modification of the formation ratio resulted in a change in DHNK and HNK clearances and HNK peripheral volume of distribution proportional to the different ratios used for DHNK and HNK formation, no effects on the objective function were observed. Third, the 5-h sampling time may have been sufficient for reliable estimation of ketamine and norketamine model parameters, but as indicated above, this time profile may have been insufficient to properly characterize the pharmacokinetics of the secondary ketamine metabolites. Sampling up to 24-48 hours post-dose would be likely to obtain sufficient data on secondary metabolite kinetics. Possibly, the estimate of the high DHNK elimination clearance estimate was related to this issue. Since no second compartment could be estimated for DHNK, no intercompartmental clearance parameter was estimated. Conceivably, the elimination clearance may be the sum of a (non-identified) intercompartmental clearance and the elimination clearance. Additionally, fixing the DHNK formation rate to 30% of the norketamine elimination rate may have overestimated the DHNK metabolic pathway.

CONCLUSIONS

We performed a population pharmacokinetic modeling study of ketamine and its major metabolites. Differences in pharmacokinetics between formulations and enantiomers were identified. Most importantly, we observed differences between *S*- and *R*-enantiomer elimination clearances. Another relevant observation was the absence of significant clinical effect of SNP on ketamine pharmacokinetics. This indicates that our previous finding of lesser psychotomimetic side effects when racemic ketamine is combined with SNP is not pharmacokinetically driven.[13] Despite some limitations, our model is likely to be of sufficient quality to be used in future pharmacokinetic and pharmacodynamic studies into the efficacy and side effects of ketamine and metabolites.

REFERENCES

1. Zanos P, Moaddel R, Morris PJ, Riggs LM, Highland JN, Georgiou P, Pereira EFR, Albuquerque EX, Thomas CJ, Zarate CA, Gould TD: Ketamine and Ketamine Metabolite Pharmacology: Insights into Therapeutic Mechanisms. Pharmacological Reviews 2018; 70: 621-660
2. Kamp J, Van Velzen M, Olofsen E, Boon M, Dahan A, Niesters M: Pharmacokinetic and pharmacodynamic considerations for NMDA-receptor antagonist ketamine in the treatment of chronic neuropathic pain: an update of the most recent literature. Expert Opin Drug Metab Toxicol. 2019; 15: 1033-1041
3. Mion G, Villevieille T: Ketamine Pharmacology: An Update (Pharmacodynamics and Molecular Aspects, Recent Findings). CNS Neurosci Ther 2013; 19: 370-380
4. Kaufman MB: Pharmaceutical Approval Update. Pharm Ther 2019; 44: 251-254
5. Zanos P, Moaddel R, Morris PJ, Riggs LM, Highland JN, Georgiou P, Pereira EFR, Albuquerque EX, Thomas CJ, Zarate CA, Gould TD: Ketamine and Ketamine Metabolite Pharmacology: Insights into Therapeutic Mechanisms. Pharm Rev 2018; 70: 621-660
6. Yanagihara Y, Kariya S, Ohtani M, Uchino K, Aoyama T, Yamamura Y, T I: Involvement of CYP2B6 in n-demethylation of ketamine in human liver microsomes. Drug Metab Dispos 2001; 29: 887-890
7. Schuttler J, Stanski DR, White PF, Trevor AJ, Horai Y, Verotta D, Sheiner LB: Pharmacodynamic modeling of the EEG effects of ketamine and its enantiomers in man. J Pharmacokinet Biopharm 1987; 15: 241-53
8. Hijazi Y, Boulieu R: Contribution of CYP3A4, CYP2B6, and CYP2C9 Isoforms to N-Demethylation of Ketamine in Human Liver Microsomes. Drug Metab Dispos 2002; 30: 853-858
9. Noppers I, Olofsen E, Niesters M, Aarts L, Mooren R, Dahan A, Kharasch E, Sarton E: Effect of rifampicin on S-ketamine and S-norketamine plasma concentrations in healthy volunteers after intravenous S-ketamine administration. Anesthesiology 2011; 114: 1435-1445
10. Kroin JS, Das V, Moric M, Buvanendran A: Efficacy of the ketamine metabolite (2R,6R)-hydroxynorketamine in mice models of pain. Reg Anesth Pain Med 2019; 44: 111-117
11. Lumsden EW, Troppoli TA, Myers SJ, Zanos P, Aracava Y, Kehr J, Lovett J, Kim S, Wang F-H, Schmidt S, Jenne CE, Yuan P, Morris PJ, Thomas CJ, Zarate CA, Moaddel R, Traynelis SF, Pereira EFR, Thompson SM, Albuquerque EX, Gould TD: Antidepressant-relevant concentrations of the ketamine metabolite (2R,6R)-hydroxynorketamine do not block NMDA receptor function. Proceedings of the National Academy of Sciences 2019; 116: 5160-5169
12. Zhao X, Venkata SL, Moaddel R, Luckenbaugh DA, Brutsche NE, Ibrahim L, Zarate CA, Jr., Mager DE, Wainer IW: Simultaneous population pharmacokinetic modelling of ketamine and three major metabolites in patients with treatment-resistant bipolar depression. Br J Clin Pharmacol 2012; 74: 304-314
13. Jonkman K, van der Schrier R, van Velzen M, Aarts L, Olofsen E, Sarton E, Niesters M, Dahan A: Differential role of nitric oxide in the psychedelic symptoms induced by racemic ketamine and esketamine in human volunteers. Br J Anaesth 2018; 120: 1009-1018

14. Sigtermans M, Dahan A, Mooren R, Bauer M, Kest B, Sarton E, Olofsen E: S(+)-ketamine effect on experimental pain and cardiac output: a population pharmacokinetic-pharmacodynamic modeling study in healthy volunteers. Anesthesiology 2009; 111: 892-903

15. Beal SL: Ways to fit a PK model with some data below the quantification limit. J Pharmacokinet Pharmacodyn 2001; 28: 481-504

16. Lindbom L, Pihlgren P, Jonsson EN: PsN-Toolkit--a collection of computer intensive statistical methods for non-linear mixed effect modeling using NONMEM. Computer Methods and Programs in Biomedicine 2005; 79: 241-57

17. Peltoniemi MA, Hagelberg NM, Olkkola KT, Saari TI: Ketamine: A Review of Clinical Pharmacokinetics and Pharmacodynamics in Anesthesia and Pain Therapy. Clin Pharmacokinet 2016; 55: 1059-1077

18. Goldberg ME, Torjman MC, Schwartzman RJ, Mager DE, Wainer IW: Enantioselective Pharmacokinetics of (R)- and (S)-Ketamine After a 5-Day Infusion in Patients with Complex Regional Pain Syndrome. Chirality 2011; 23: 138–143

19. Geisslinger G, Hering W, Thomann P, Knoll R, Kamp HD, Brune K: Pharmacokinetics and Pharmacodynamics of ketamine enantiomers in surgical patients using a stereoselective analytical method. Br J Anaesth 1993; 70: 666-671

20. Ihmsen H, Geisslinger G, Schuttler J: Stereoselective pharmacokinetics of ketamine: R(-)-ketamine inhibits the elimination of S(+)-ketamine. Clin. Pharmacol. Ther. 2001; 70: 431-8

21. Henthorn TK, Avram MJ, Dahan A, Gustafsson LL, Persson J, Krejcie TC, Olofsen E: Combined Recirculatory-compartmental Population Pharmacokinetic Modeling of Arterial and Venous Plasma S(+) and R(-) Ketamine Concentrations. Anesthesiology 2018; 129: 260-270

22. Moaddel R, Sanghvi M, Dossou KSS, Ramamoorthy A, Green C, Bupp J, Swezey R, O'Loughlin K, Wainer IW: The distribution and clearance of (2S,6S)-hydroxynorketamine, an active ketamine metabolite, in Wistar rats. Pharm Res Per 2015; 3: 1-10

SUPPLEMENTAL DATA

Supplemental Table 1. Mean peak concentrations of individual analytes

Analyte	C_{MAX} ± SD (nmol/mL)	T_{MAX} ± SD (min)
Esketamine		
S-Ketamine	1.111 ± 0.160	170 ± 19
S-Norketamine	0.876 ± 0.130	187 ± 5
S-DHNK	0.050 ± 0.018	270 ± 45
S-HNK	0.221 ± 0.058	251 ± 59
Racemic ketamine		
S-Ketamine	1.115 ± 0.105	173 ± 18
S-Norketamine	0.840 ± 0.107	190 ± 12
S-DHNK	0.054 ± 0.018	253 ± 57
R-Ketamine	1.211 ± 0.117	170 ± 19
R-Norketamine	0.975 ± 0.134	187 ± 9
R-DHNK	0.099 ± 0.032	290 ± 30
RS-HNK*	0.363 ± 0.125	242 ± 56

Maximum concentrations of the individual isomers after administration of either esketamine or racemic ketamine. C_{MAX} = mean peak concentration; SD = standard deviation; T_{MAX} = mean time at which concentration is C_{MAX}. *Total HNK concentration.

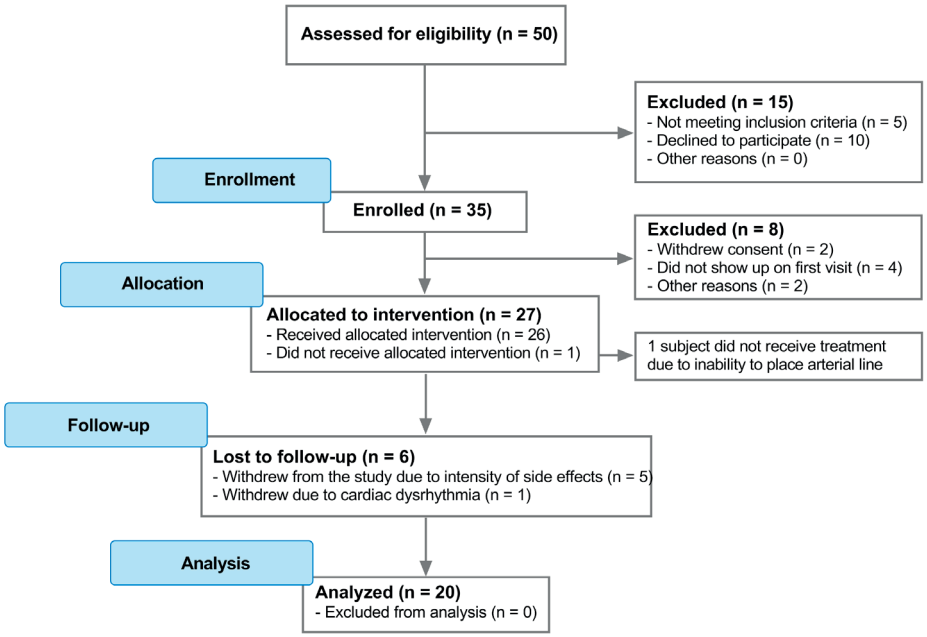

Supplemental Figure 1. Consort flowchart

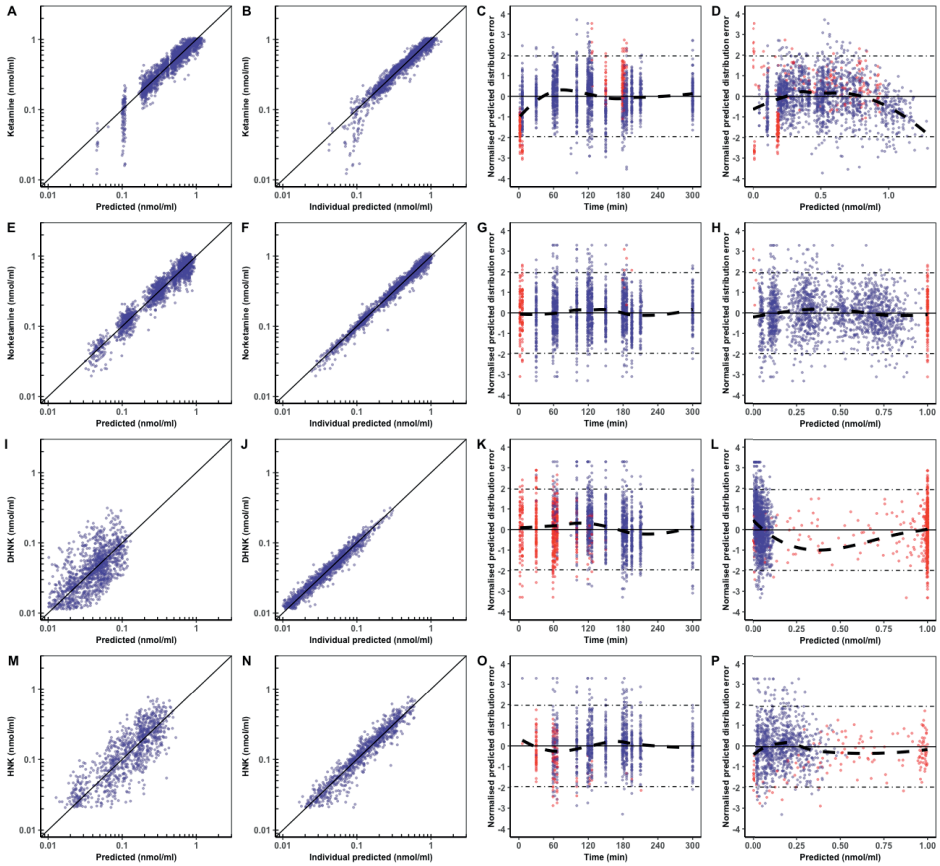

Supplemental Figure 2. Goodness of fit plots. Predicted *versus* measured data, individual predicted *versus* measured data, normalized prediction distribution error *versus* time and normalized prediction distribution error *versus* predicted plots for pooled ketamine (**A-D**), norketamine (**E-H**), DHNK (**I-L**) and HNK (**M-P**) data. Data points below the lower limit of quantitation and above the upper limit of quantitation are shown in red in the normalized prediction distribution error panels.

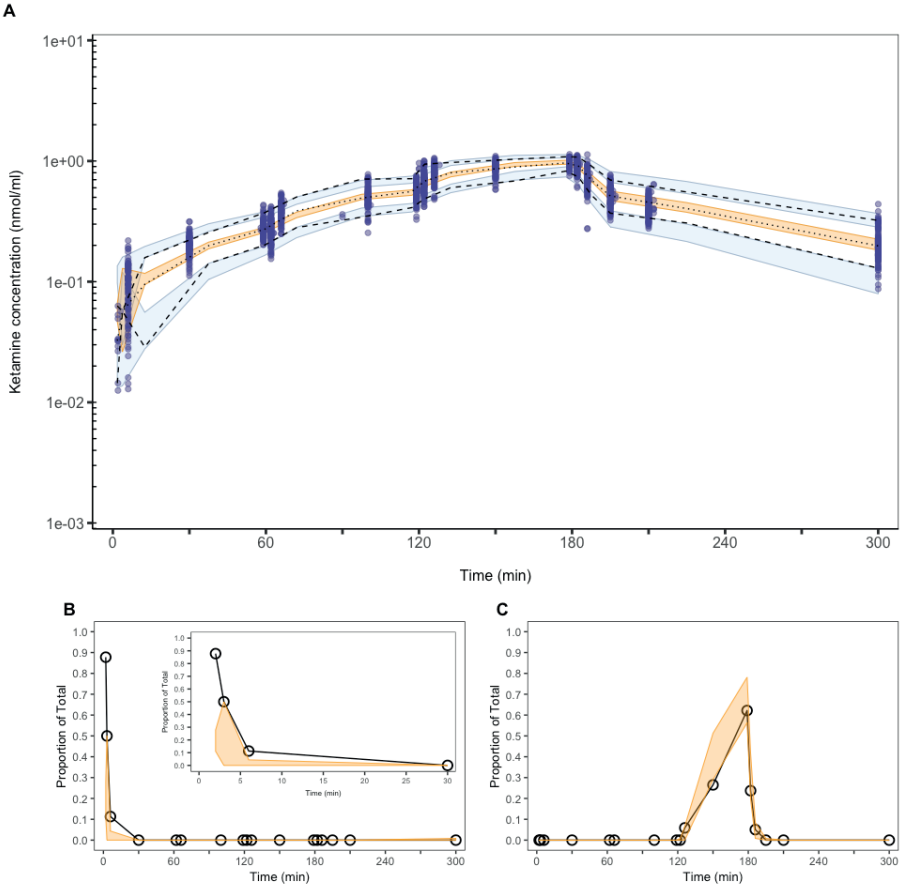

Supplemental Figure 3. Prediction-variance-corrected visual predictive checks for pooled ketamine data (**A**). The dots represent the observed data. The dashed lines represent the 5th and 95th percentiles of the observed data. The median of the observed data is shown by the dotted line. The 95% prediction intervals of the 5th and 95th percentiles and median of the simulated data are shown by the shaded areas. Visual predictive checks for data below the limit of quantitation (**B**) and above the upper limit of quantitation (**C**). The black dots and line represent the proportion BLQ (**B**) or ULOQ (**C**) data points in the observed data. The 95% prediction interval of the proportion in the simulated data is shown by the shaded area.

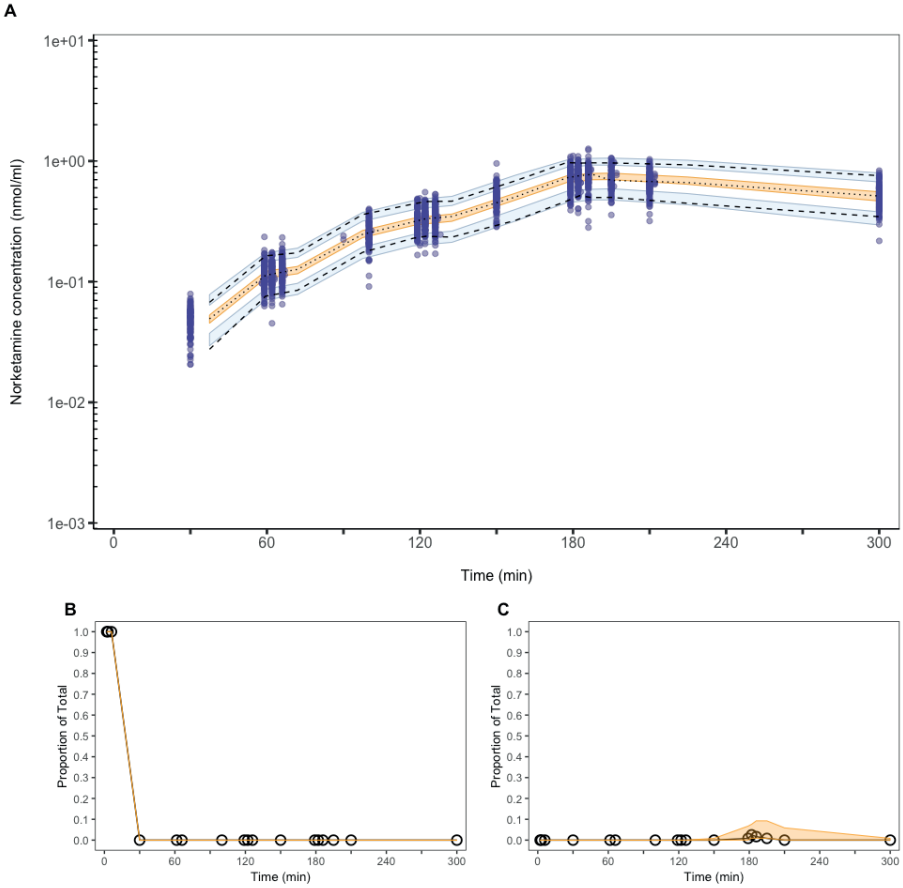

Supplemental Figure 4. Prediction-variance-corrected visual predictive checks for pooled norketamine data (**A**). The dots represent the observed data. The dashed lines represent the 5th and 95th percentiles of the observed data. The median of the observed data is shown by the dotted line. The 95% prediction intervals of the 5th and 95th percentiles and median of the simulated data are shown by the shaded areas. Visual predictive checks for data below the limit of quantitation (**B**) and above the upper limit of quantitation (**C**). The black dots and line represent the proportion BLQ (**B**) or ULOQ (**C**) data points in the observed data. The 95% prediction interval of the proportion in the simulated data is shown by the shaded area.

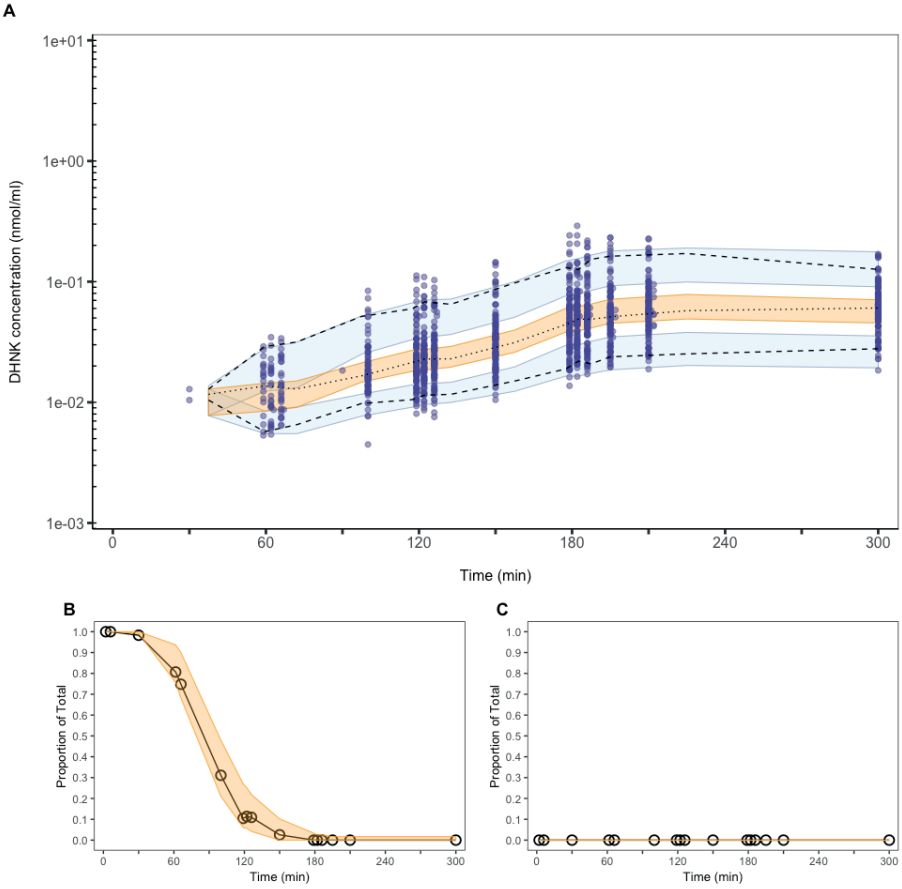

Supplemental Figure 5. Prediction-variance-corrected visual predictive checks for pooled dehydronorketamine data (**A**). The dots represent the observed data. The dashed lines represent the 5th and 95th percentiles of the observed data. The median of the observed data is shown by the dotted line. The 95% prediction intervals of the 5th and 95th percentiles and median of the simulated data are shown by the shaded areas. Visual predictive checks for data below the limit of quantitation (**B**) and above the upper limit of quantitation (**C**). The black dots and line represent the proportion BLQ (**B**) or ULOQ (**C**) data points in the observed data. The 95% prediction interval of the proportion in the simulated data is shown by the shaded area.

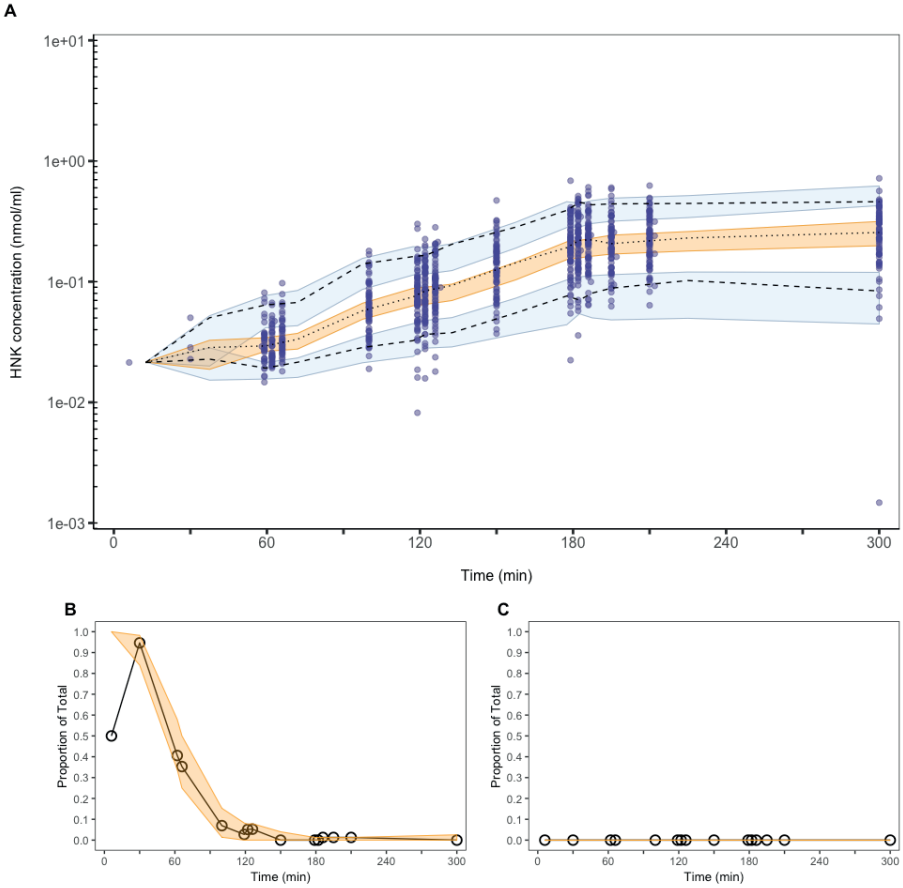

Supplemental Figure 6. Prediction-variance-corrected visual predictive checks for pooled hydroxynorketamine data (**A**). The dots represent the observed data. The dashed lines represent the 5th and 95th percentiles of the observed data. The median of the observed data is shown by the dotted line. The 95% prediction intervals of the 5th and 95th percentiles and median of the simulated data are shown by the shaded areas. Visual predictive checks for data below the limit of quantitation (**B**) and above the upper limit of quantitation (**C**). The black dots and line represent the proportion BLQ (**B**) or ULOQ (**C**) data points in the observed data. The 95% prediction interval of the proportion in the simulated data is shown by the shaded area.